

Aggregation-disaggregation transition of DNA-coated colloids: Experiments and theoryRémi Dreyfus,^{1,*} Mirjam E. Leunissen,^{1,†} Roujie Sha,² Alexei Tkachenko,³ Nadrian C. Seeman,² David J. Pine,¹ and Paul M. Chaikin¹¹*Center for Soft Matter Research, New York University, New York, New York 10003, USA*²*Chemistry Department, New York University, New York, New York 10003, USA*³*Center for Functional Nanomaterials, Brookhaven National Laboratory, Building 735, Upton, New York 11973, USA*

(Received 18 December 2009; published 23 April 2010)

Colloids coated with complementary single-stranded DNA “sticky ends” associate and dissociate upon heating. Recently, microscopy experiments have been carried out where this association-dissociation transition has been investigated for different types of DNA and different DNA coverages [R. Dreyfus, M. E. Leunissen, R. Sha, A. V. Tkachenko, N. C. Seeman, D. J. Pine, and P. M. Chaikin, *Phys. Rev. Lett.* **102**, 048301 (2009)]. It has been shown that this transition can be described by a simple quantitative model which takes into account the features of the tethered DNA on the particles and unravels the importance of an entropy cost due to DNA confinement between the surfaces. In this paper, we first present an extensive description of the experiments that were carried out. A step-by-step model is then developed starting from the level of statistical mechanics of tethered DNA to that of colloidal aggregates. This model is shown to describe the experiments with excellent agreement for the temperature and width of the transition, which are both essential properties for complex self-assembly processes.

DOI: [10.1103/PhysRevE.81.041404](https://doi.org/10.1103/PhysRevE.81.041404)

PACS number(s): 82.70.Dd, 81.16.Dn

I. INTRODUCTION

DNA-mediated nano-microstructure systems of particles have been the subject of intense research recently due to their potential applications in self-assembly or molecular recognition [1–3]. For self-assembly processes, DNA-coated nanoparticles are very promising materials as DNA provides specific interactions. Such a method was recently used successfully to generate ordered crystalline structures such as bcc and fcc [4–6]. Creating such ordered structures requires the particles to find their equilibrium positions. Therefore, it is important to understand precisely the association-dissociation behavior of DNA-coated colloids. Such an understanding will further be useful in designing self-assembled structures. Despite a considerable amount of experimental [4,7–18] and theoretical work [11,12,19–24], a clear quantitative description of the association-dissociation process has just begun to emerge, as well as a clear comparison to experiments [25]. In this paper, the first part consists of a description of experiments performed in order to investigate this transition. In the second part, a theoretical model of the association-dissociation transition of DNA-coated colloids is proposed. The third part is a comparison between the model and the experiments. Finally, the reader interested only in using these results to design systems with specific DNA-mediated interactions can skip to Sec. V where all the formulas needed to engineer such systems are summarized.

II. EXPERIMENTAL PART**A. Measurement of the association-dissociation transition**

The experimental system under investigation was a mixture of complementary colloidal particles of 525 nm radius. Each particle carried DNA construct consisting of double-stranded DNA containing 49 base pairs, at the end of which was a “sticky end:” a single-stranded DNA sequence with 11 bases. Each complementary pair of colloids had sticky ends that could hybridize to form a double strand which bound the particles together. There were $\sim 22 \cdot 10^4$ DNA constructs bound to the surface of each particle. When complementary colloids were mixed in solution, there was a temperature, the dissociation temperature T_d , below which complementary colloids aggregated (Fig. 1). When the sample was heated above T_d , particles did not stick together and remained suspended in solution as singlets (Fig. 1). Around the dissociation temperature, there was an equilibrium where particles could either remain in a cluster or as singlets in solution. In order to experimentally observe the dissociation temperature, the fraction of singlets f was measured as a function of temperature on a temperature gradient. The temperature gradient was generated on the light microscope using a copper plate, one end of which was connected to a Peltier heating element

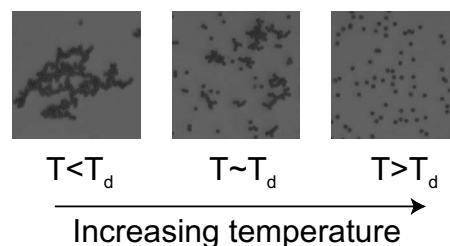


FIG. 1. Transition from an aggregated to a disaggregated state of DNA-coated colloids upon heating.

*Present address: Complex Assemblies of Soft Matter, CNRS-Rhodia-UPenn UMI 3254, Bristol, Pennsylvania 19007, USA; remi.dreyfus@gmail.com

†Present address: FOM Institute AMOLF, Science Park 104, 1098 XG Amsterdam, The Netherlands.

while the other end was cooled by a thermostatted water bath. After 1 h equilibration time, the suspension confined to a $100 \times 2.0 \times 0.1$ mm glass capillary—Vitrocom—on top of a silicon wafer was imaged in reflection, going from a fully aggregated state at the “cold” end to a fully dissociated state at the “hot” end. As our colloids were 1.7 times denser than water, their sedimentation resulted essentially in a two-dimensional system (Fig. 1). For each point, we measured the fraction of nonaggregated particles, or “singlet fraction,” by videomicroscopy [26]. The temperature gradient inside the capillary was constant at about 0.7 °C/cm and the measured uncertainty is ± 0.2 °C at each point. The measured dissociation curves were independent of equilibration times and steepness of the temperature gradient.

B. Materials and methods, characterization

1. Materials and methods

The DNA construct consisted of a 61-nucleotide-long oligomer (IDT, Coralville, IA), attached via a short poly(ethylene glycol) spacer to a 5' biotin group and hybridized from its 5'-end to a 49-nucleotide complementary strand (CS). The hybridization was done at equimolar strand ratios and an overall DNA concentration of 15 μ M (UV-260 absorption, Genequant spectrometer) in 50 mM phosphate/ 50 mM NaCl hybridization buffer (pH 7.5) by slowly cooling down from 90 to 22 °C in a water bath. The result was a rigid ~ 15 -nm-long double-stranded “rod” with a flexible single-stranded end of 11 bases. We used three types of ends, two of which were complementary “sticky” sequences $S(S')$; the other was a “nonsticky” thymine-only sequence (T). 1.05 μ m diameter polystyrene Dynabeads (MyOne Streptavidin C1, Molecular Probes) were coated with T and $S(S')$ DNAs in the ratio $\gamma = n_S / (n_S + n_T)$, where n_S and n_T were, respectively, the numbers of $S(S')$ and T DNA strands per bead. This was achieved by combining 5 μ l of bead suspension with 10 μ l of a DNA solution and 60 μ l of suspension buffer (10 mM phosphate/ 50 mM NaCl and 0.5 wt % Pluronic surfactant, pH 7.5) and allowing this mixture to incubate for 30 min at room temperature. To remove excess and nonspecifically adsorbed DNA, the particles were centrifuged and resuspended 3 times in 100 μ l suspension buffer; we repeated this washing procedure twice, heating in between for 30 min at 55 °C (this is below the CS melting temperature of ~ 70 °C at 1 μ M). The final colloidal system obtained is shown schematically in Fig. 2.

2. Characterization of particle coverage

For radioactive determination of the DNA coverage, part of the CS-DNA was labeled with a 32 P isotope and mixed with unlabeled CS-DNA in a known number ratio ($\sim 1:1000$) before hybridization with S -DNA; T -DNA was hybridized with unlabeled CS-DNA only. After incubation and washing, the number of decay events was determined with an Intertechnique SL30 scintillation counter and related to the number of DNA strands per particle. As expected, the number of tethered $S(S')$ sticky ends depended linearly on the mixing ratio γ of S and T strands (Fig. 3). Furthermore,

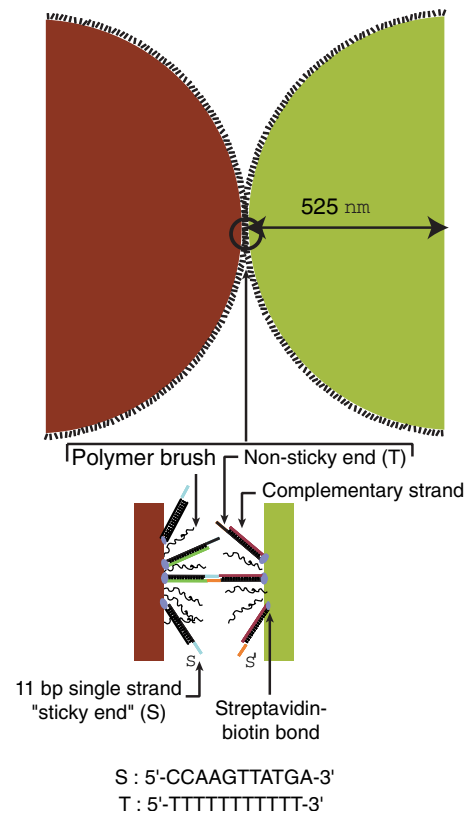


FIG. 2. (Color) Representation of the experimental system consisting of micrometer-sized particles coated with a sterically stabilizing polymer brush and a mix of sticky and nonsticky DNAs.

our washing procedure indeed eliminated initial nonspecific adsorption, with the coverage reaching a constant value of $\sim 2.2 \times 10^4$ strands per particle after two washing cycles (inset in Fig. 3). The influence of the incubation time on the DNA coverage was also investigated. Figure 4 showed that, for the concentration of particles and DNA used, all the DNAs were adsorbed after 20 min, which was the reason why an incubation time of 30 min was chosen in our experiments.

These measurements gave us a good estimate of the number of DNA strands per particle N_{DNA} and the surface den-

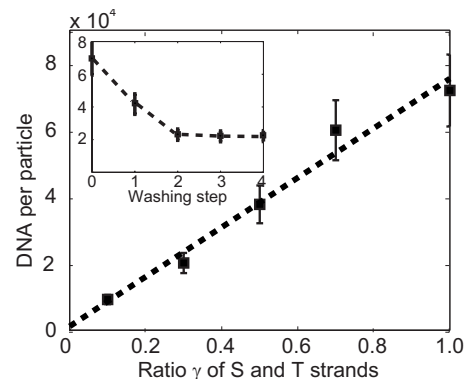


FIG. 3. Number of DNA per particle as a function of the mixing ratio γ of S and T strands. Inset shows the desorption of nonspecifically bound DNA from the surface as a function of the number of heating-washing cycles.

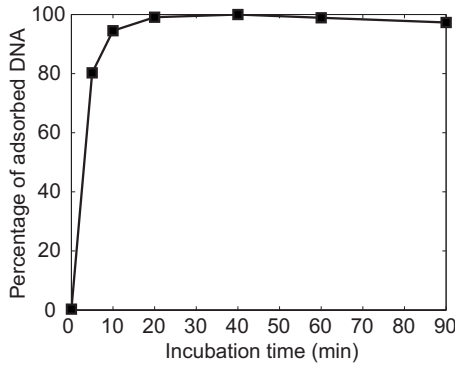


FIG. 4. Kinetics of adsorption of DNA at the surface of colloids.

sity, $\rho = \frac{N_{\text{DNA}}}{4\pi a^2}$. There were approximately 22 000 strands per particle, which corresponded to a surface density of $\sim 6.4 \times 10^{-3}$ DNA/nm². The average spacing between two tethered DNAs on a surface was ~ 12.5 nm.

3. Thermodynamic parameters of DNA suspended in solution

Whereas earlier studies relied on predictions from nearest-neighbor thermodynamics [27], in this study, the actual hybridization free energy ΔG^0 was determined by measuring the dehybridization curves of the 11 bp sticky end sequences with UV-260 absorption at different concentrations. 1:1 *S-S'* solutions in the suspension buffer were prepared at different overall concentrations c_{tot} of 2.3, 4.1, 6.6, and 13 μM and hybridized by cooling from 90 to 8 $^{\circ}\text{C}$ at a rate of ~ 0.25 $^{\circ}\text{C}/\text{min}$. Since single-stranded DNAs have a stronger absorption in the UV range than double-stranded DNA, the dehybridization curve was obtained by measuring the change of the DNA optical density (OD) as a function of temperature (inset in Fig. 5). In our experiments, the temperature was ramped up at 0.25 $^{\circ}\text{C}/\text{min}$ and a DNA-free buffer served as the baseline measurement. The change of OD as a function of temperature allowed us to measure the melting temperature T_m of the complementary sticky ends for different overall strand concentration c_{tot} . It is known from

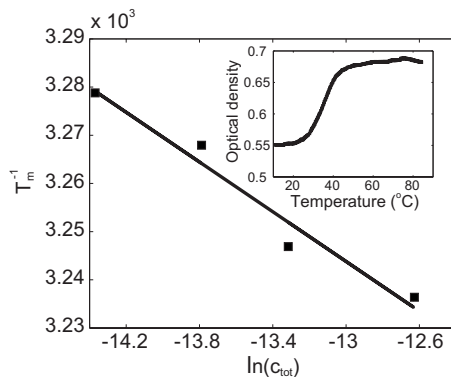


FIG. 5. Linear relation between T_m^{-1} and $\ln(c_{\text{tot}})$. The thermodynamics parameters are inferred from the slope and the intercept. Inset shows a typical dehybridization curve of sticky ends in solution.

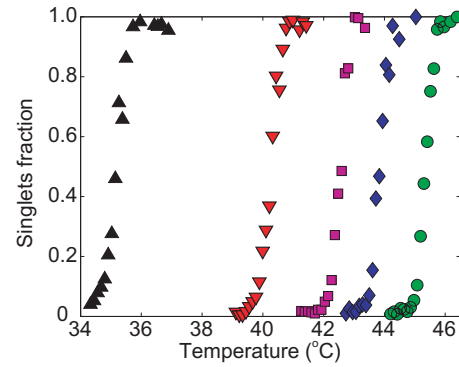


FIG. 6. (Color) Particle singlet fraction as a function of temperature for sticky end fraction $\gamma=0.2$ (black triangles), $\gamma=0.4$ (red inverted triangles), $\gamma=0.6$ (magenta squares), $\gamma=0.8$ (blue diamonds), and $\gamma=1$ (green dots).

Ref. [28] that the melting temperature depends on the overall concentration following

$$T_m = \frac{\Delta H^0}{\Delta S^0} - \frac{\Delta H^0}{R} \ln\left(\frac{c_{\text{tot}}}{4c^0}\right), \quad (1)$$

where $c^0=1$ mol/l is a standard concentration. The measured T_m is plotted as a function of $\ln(c_{\text{tot}})$ in Fig. 5 for the sticky ends. The slope and intercept of the linear fit give us both the enthalpy of hybridization $\Delta H^0 = -322$ kJ/mol and the entropy of hybridization $\Delta S^0 = -936$ J/mol K of the sticky ends.

C. Results and discussion

Figure 6 shows the experimentally obtained dissociation curves for our particles with sticky end ratios in the range of $\gamma=0.2-1.0$, which corresponds to an average spacing between the sticky ends ranging from 12 to 28 nm. The experimental results show that the dissociation temperature increases when the coverage on the particles increases. This is expected as the number of potential DNA bonds determines the strength of the attractive potential between the particles. The dissociation curves are very sharp. Sharp curves have already been measured for DNA-coated nanoparticles [7]. It was shown that, in those experiments, cooperative melting of tightly packed DNA duplexes [13] or entropic cooperativity of the DNA-particle network [20] contributes to the sharpness of the transition. However, such an explanation does not apply to our experiments because there are no free DNA linkers in solution and the average spacing between the sticky ends is much larger than that on nanoparticles. Another surprising fact is the weak dependence of the width of the transition on the coverage ratio. This fact is surprising as one might expect intuitively that the binding free energy ΔG_p of the particles is given by

$$\Delta G_p \approx N_p \Delta G^0 = N_p (\Delta H^0 - T \Delta S^0), \quad (2)$$

with the values of ΔH^0 and ΔS^0 as measured in solution (see above) and N_p is the number of potential bonds between the particles. When the binding free energy equals the entropy change between unbound, $R \ln(C_u)$, and bound particles,

$R \ln(1/v_b)$, the particles should dissociate. Here, C_u is the concentration of unbound particles and v_b is the volume around a particle over which it interacts with neighboring particles, corresponding to the range of the DNA-mediated attraction. The dissociation transition can be considered to be complete when the entropy change per singlet is about twice the binding free energy $R(T_d + \delta T) \ln(v_b C_u/2) \approx 2\Delta G_p(T_d + \delta T)$. In this simplistic model, the dissociation temperature and width of the transition are then given by

$$T_d \approx \frac{\Delta H^0}{\left(\Delta S^0 + \frac{R \ln(v_b C_u/4)}{N_p}\right)}, \quad 2\delta T \approx -\frac{RT_d \ln(v_b C_u/2)}{N_p \Delta S^0}. \quad (3)$$

For this model, the temperature below which the DNA-mediated particle interaction is attractive, $T_0 = \frac{\Delta H^0}{\Delta S^0}$, remains the same as for the free DNA in solution. However, it can be readily seen that when the number N_p of simultaneously formed DNA bonds increases, the dissociation temperature increases and the width of the transition decreases. Both the dissociation temperature and the sharpness of the transition are intimately related in the framework of such a model. For our system, the temperature below which the particles should remain attractive is $T_0 \sim 71$ °C, which is far above the experimentally observed dissociation temperature of the aggregates. Moreover, the sharpness of the transition remains almost the same though the coverage changes by a factor 5. These discrepancies suggest that a more elaborate model should be developed, which is the subject of the next section.

III. THEORETICAL PART

A. Presentation of the problem

In this section, we develop the equations which relate the dissociation curves for our DNA-coated particles to the measured melting curves of the individual DNA sticky ends in solution. The basic ingredients are:

(a) Finding the effective particle—particle interaction:

(1) Determination of the hybridization free energy ΔF_{tether} of the tethered sticky end bonds, which includes the calculation of an additional per bond entropic cost from the constraints in joining together the freely pivoting DNA strands on each particle.

(2) An entropic gain from the combinatorics of DNA from one particle binding to several complementary strands on another particle.

(3) An entropic loss or repulsion from unbound DNA on one particle encountering the surface of the complementary particle.

(b) Predicting the number of singlet particles in a suspension with the above interactions.

B. From hybridization free energy of DNA in solution to hybridization free energy of an interparticle bond

At low temperature, the attraction that drives the colloidal association results from the hybridization of the complementary sticky ends tethered to the surface of the particles. The

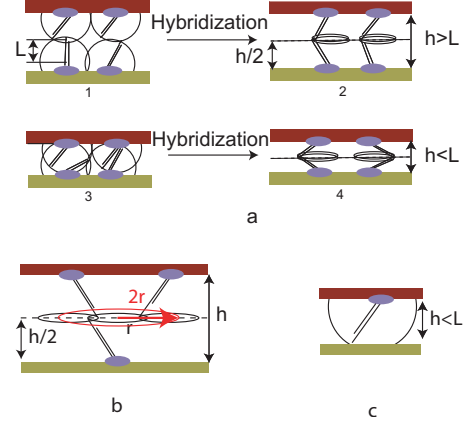


FIG. 7. (Color) (a) Motion restriction of hybridized tethered DNA bonds. (b) Basic geometry used to calculate the number of k choices a DNA has to bind to a strand on the opposite surface. (c) Motion restriction of nonhybridized tethered DNA due to the opposite particle.

hybridization free energy of DNA strands that are attached to a surface differs from the hybridization free energy of free DNA in solution due to confinement effects. While the hybridized DNA in solution can explore the same volume as the unhybridized strands, the freedom of motion of a pair of hybridized DNA tethers on the colloid surface is strongly restricted, as compared to the unhybridized case [Fig. 7(a)]. Indeed, before DNA strands are hybridized, DNA can rotate around their attachment point. Therefore, unhybridized strands can explore the surface of half a sphere [Fig. 7(a), part 1] or half a truncated sphere [Fig. 7(a), part 3], depending on the separation between the colloid surfaces. After hybridization, strands can only explore a circle [Fig. 7(a), parts 2–4]. This restriction gives rise to an additional configurational entropy penalty. We can derive an approximate expression for the hybridization free energy of tethered DNA by considering the partition functions for the hybridization equilibrium of free DNA in solution and for the hybridization between two flat surfaces. In general, the partition function Q for a system of N indistinguishable objects can be written as

$$Q(N, V, T) = \frac{1}{\Lambda^{3N} N!} \int dr^{3N} \exp[-\beta U(r^N)], \quad (4)$$

with the thermal De Broglie wavelength $\Lambda = \sqrt{h^2/2\pi mkT}$. For free DNA in solution, this simplifies to

$$Q_x(N, V, T) = \frac{V_x^{N_x}}{\Lambda_x^{3N_x} N_x!} q_{\text{int},x}^{N_x}, \quad (5)$$

where $x = S, S', SS'$ and $q_{\text{int},x}$ is the contribution due to all internal degrees of freedom. Via $F_x = -RT \ln Q_x$, $\mu_x = \left(\frac{\partial F_x}{\partial N_x}\right)_{T,V}$, the equilibrium condition $\mu_S + \mu_{S'} = \mu_{SS'}$, the concentration $C_x = N_x/V$, and the fact that all species explore the same volume, i.e., $V_S = V_{S'} = V_{SS'} = V$, we arrive at

$$\frac{C_{SS'}}{C_S C_{S'}} = \frac{q_{int,SS'}/\Lambda_{SS'}^3}{q_{int,S}q_{int,S'}/\Lambda_S^3\Lambda_{S'}^3} = \frac{K_{eq}}{c^0}, \quad (6)$$

where $c^0=1$ mol/l is a standard concentration and K_{eq} is the reaction constant of the DNA hybridization reaction. Let us now consider the hybridization of two DNA strands that are attached to opposing colloidal surfaces. The hybridization free energy for such a tethered pair is

$$\Delta F_{tether} = -RT \ln\left(\frac{Q_{bound}}{Q_{unbound}}\right), \quad (7)$$

where $Q_{bound}=Q_{SS'}$ and $Q_{unbound}=Q_S Q_{S'}$. Using the general expression of Eq. (5) and from a comparison to Eq. (6), it follows that

$$\frac{Q_{bound}}{Q_{unbound}} = \frac{V_b}{V_u^2} \frac{q_{int,SS'}/\Lambda_{SS'}^3}{q_{int,S}q_{int,S'}/\Lambda_S^3\Lambda_{S'}^3} = \frac{V_b K_{eq}}{V_u^2 c^0}, \quad (8)$$

where $V_u=V_S=V_{S'}$ and $V_b=V_{SS'}$. Thus, the hybridization free energy for a tethered strand is [Eq. (7)]

$$\Delta F_{tether} = \Delta G^0 - RT \ln \frac{V_b}{V_u^2 c^0}, \quad (9)$$

where ΔG^0 is the hybridization free energy of the strands when freely suspended in solution and the last term is the configurational entropy penalty ΔS_p due to confinement between the colloid surfaces. According to Fig. 7, two different cases must be considered when calculating these terms.

For a surface separation $h < L$,

$$V_u = 2\pi Lh \quad V_b = 2\pi L \sqrt{1 - \left(\frac{h}{2L}\right)^2}. \quad (10)$$

For a surface separation $h > L$,

$$V_u = 2\pi L^2 \quad V_b = 2\pi L \sqrt{1 - \left(\frac{h}{2L}\right)^2}. \quad (11)$$

For two strands that exactly oppose each other on two different surfaces, we find the following approximate expression for the entropy penalty ΔS_p :

$$\Delta S_p = R \ln\left(\frac{2\pi Lh^2 c^0}{\sqrt{1 - \left(\frac{h}{2L}\right)^2}}\right) \text{ for } h < L, \quad (12)$$

$$\Delta S_p = R \ln\left(\frac{2\pi L^3 c^0}{\sqrt{1 - \left(\frac{h}{2L}\right)^2}}\right) \text{ for } h > L. \quad (13)$$

The hybridization free energy ΔF_{tether} for a tethered strand becomes

$$\Delta F_{tether} = \Delta H^0 - T(\Delta S^0 + \Delta S_p). \quad (14)$$

The variation of $\frac{\Delta S_p}{R}$ is shown in Fig. 8.

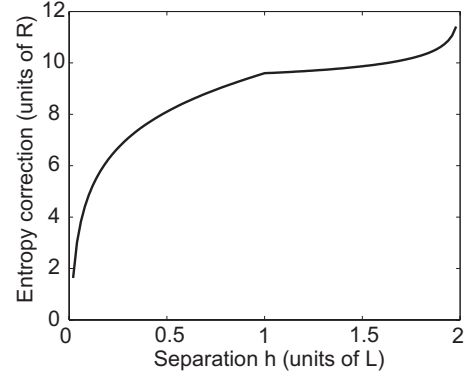


FIG. 8. Entropy correction as a function of the particle separation (solid line).

C. Effective interparticle interaction

1. DNA-mediated attraction

The DNA-mediated attraction depends strongly on the number of potential bonds N_p that particles can form. This number depends on the surface to surface separation h . The number of potential bonds particles can form is the product of the surface density of sticky DNA $\rho_s = \gamma\rho$ and the adhesion area $S_A = \pi a(2L-h)$, which corresponds to the overall area on which two strands on complementary particles can geometrically hybridize. L is the length of the DNA strand. The number of possible bonds is $N_p = \frac{\gamma N_{DNA}}{4a}(2L-h) \approx 31-154$ for a mixing ratio $\gamma=0.2-1$ and a typical separation $h=L$. Since we study a system with relatively short DNA, as compared to the particle radius, the curvature of the particles is now neglected. Two interacting particles are considered as being two plates, each plate having on its surface a number of DNA strands equal to the number N_p of strands in the adhesion patch of the particles previously calculated. The DNA construct used in the experiments is such that there is a flexible polyethylene glycol (PEG) linker between the biotin and the streptavidin. Therefore, the DNA is supposed to rotate freely around its attachment point [Fig. 7(b)]. The spacing between the DNAs is small enough (~ 12.5 nm from radioactivity measurement) that a DNA on a surface can bind to more than one DNA on the opposite surface. We denote by k the number of DNA to which a DNA on the opposite surface can bind geometrically. k is estimated by $k=4\pi[L^2 - (\frac{h}{2})^2]\rho\gamma$. In the case where $h \sim L$, for $\gamma=1$, $k \sim 13$. This k factor must be taken into account in the calculation of the partition function Z_p for two interacting plates covered with DNA. Indeed, there are $\binom{N_p}{N}$ ways to choose N DNA on one surface to form a bond of energy ΔF_{tether} . Once these DNAs are chosen, each of them has k ways of forming a bond with a DNA on the opposite surface. Therefore, the partition function Z_p for the system is

$$Z_p = \sum_{N=0}^{N_p} \binom{N_p}{N} k^N e^{-N\beta\Delta F_{tether}} = (1 + ke^{-\beta\Delta F_{tether}})^{N_p}. \quad (15)$$

Therefore, the particle binding free energy is

$$\Delta F_{p,DNA} = -RT \ln[(1 + ke^{-\beta\Delta F_{tether}})^{N_p} - 1]. \quad (16)$$

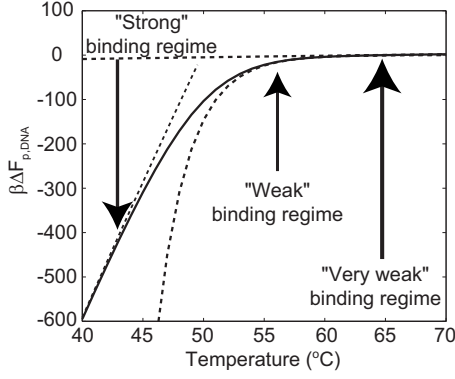


FIG. 9. Particle binding free energy as a function of temperature at fixed separation distance $h=L$.

Figure 9 shows on the same graph the particle binding free energy (solid curve) and the different binding regimes. This graph shows interesting features. In contrast to the DNA hybridization free energy, the particle binding free energy is not a linear function of the temperature, but exhibits two asymptotical linear regimes (dashed lines). At low temperature, in the regime where $ke^{-\beta\Delta F_{tether}} \gg 1$, the particle binding free energy is

$$\Delta F_{p,DNA} = N_p \Delta F_{tether} - N_p RT \ln(k). \quad (17)$$

In such a regime, particle binding is strong: the maximum number of bonds γN_p is formed with an energy ΔF_{tether} . There is an additional stabilizing term to this energy $-N_p RT \ln(k)$, which is an entropic term. This entropic term comes from the fact that each DNA may bind to k DNA on the opposing surface.

The other regime is a regime of “very weak binding.” In this regime, $N_p k e^{-\beta\Delta F_{tether}} \ll 1$. The resulting binding free energy is

$$\Delta F_{p,DNA} = \Delta F_{tether} - RT \ln(N_p k). \quad (18)$$

This very weak binding free energy corresponds to the case where only a single bond links the two particles. The energy associated is just the hybridization free energy of a single DNA ΔF_{tether} and an additional stabilizing entropic term $-RT \ln(N_p k)$, which corresponds to the fact that there are kN_p ways of forming one bond between the surfaces.

As we will show later, our experiments occur in an intermediate binding regime, which we call “weak-binding” regime (Fig. 9). In such an intermediate regime, $ke^{-\beta\Delta F_{tether}} \ll 1$ but the number of potential bonds is high enough so that $N_p k e^{-\beta\Delta F_{tether}} \gg 1$. In the weak-binding regime, each strand has a weak probability to be hybridized, but the number of bonds is so high that the probability for particles to remain associated is important. In the weak-binding regime, the binding free energy is

$$\Delta F_{p,DNA} = -RT N_p k e^{-\beta\Delta F_{tether}}. \quad (19)$$

The mean number of bonds N_{bonds} between the particles is also inferred from the partition function Z_p . The average number of bonds linking the particles together is

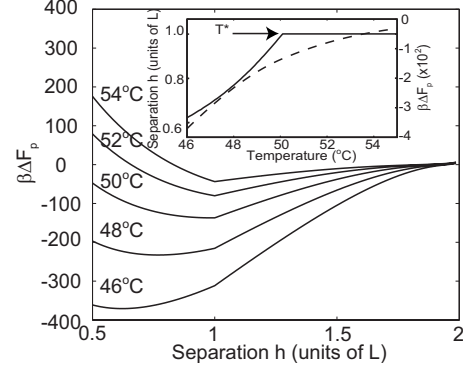


FIG. 10. Particles binding free energy profile for different temperatures. Inset shows the dependence of the equilibrium distance between the particles (solid lines) and the corresponding particles binding free energy (dashed line) as a function of temperature.

$$N_{bonds} = N_p \frac{ke^{-\beta\Delta F_{tether}}}{1 + ke^{-\beta\Delta F_{tether}}}. \quad (20)$$

This last relation shows that at low temperature in the strong-binding regime, as $ke^{-\beta\Delta F_{tether}} \gg 1$, $N_{bonds} = N_p$. At low temperature, all the possible bonds are formed. At high temperature, the number of bonds goes to 0: the particles unbind.

2. Repulsion

When the DNA-coated particles are brought together, there are repulsive forces which result from the compression of the “brushes” formed by the unbound DNA. Such a term is estimated by considering the loss of configurational entropy of unbound confined DNA. If particles are separated by a distance $h > L$ [Fig. 7(a)], the total number of configurations W of an unbound DNA is proportional to the area it explores: $W \sim 2\pi L^2$. When DNA is confined between two plates, as shown in Fig. 7(c), the number of confined configurations W_c is reduced to $W_c \sim 2\pi Lh$. The total energy ΔF_{rep} of entropic origin due to this loss of configurations is the product of the total number of DNA on both surface $2N_p$ and the repulsion energy per strand

$$\Delta F_{rep} = 2N_p RT \ln\left(\frac{L}{h}\right) \text{ for } h < L. \quad (21)$$

Figure 10 shows the variation of the particle binding free energy as a function of the distance between the particles. Here, the entropy correction, the number of potential bonds, and the factor k depend on the separation h . At low temperature, the particle binding free energy exhibits a minimum at a separation distance $h < L$. As the temperature is increased, the attraction becomes so weak that the repulsion expels the particles at a distance $h=L$ where it vanishes. Therefore, there exists a certain temperature T^* above which the minimum of particle binding free energy is obtained at a separation distance $h=L$ (inset, Fig. 10). The dashed curve in Fig. 10 shows that at the temperature where repulsion becomes dominant, the binding free energy is still 2 orders of magnitude larger than RT . At that temperature, particles dissociation does not occur. This allows us to assume in the rest of

this paper that particles remain at a distance $h=L$ and that $\Delta F_p = \Delta F_{p,\text{DNA}}(h=L)$.

3. Other sources of repulsion

There may be other sources of repulsion. For instance, particles are stabilized with a surfactant made of a PEG polymer brush. We have checked that, by changing the size of the polymer brush, the dissociation temperature of the aggregates remains the same. Therefore, the polymer does not play in our system any significant role. We also investigated another source of repulsion, which is the excluded volume interaction between the rigid double-stranded DNA. It appears to be quite small ($\approx 0.3RT$).

D. Association-dissociation transitions of colloids in aggregates

In this paragraph, we give a simple qualitative description of association-dissociation transitions of colloids in aggregates. A complete quantitative description of the association transition is given in the Appendix. Therefore, we suggest the reader to read the Appendix for more detailed information. Inside a compact aggregate, colloids interact with their z neighbors, where z is the coordination number. A particle in an aggregate, though attached to their neighbors, has the possibility to wiggle in a certain area, A_w . In the cell model developed by Sear [29], the wiggling area is such that $A_w \approx (\frac{l}{2})^2$, where l is the width of the interparticle potential [30]. As the particle can explore different states in this wiggling area while interacting with the neighbors, there is an entropy associated to the particles equal to $R \ln(\frac{A_w}{\Lambda^2})$, where Λ^2 corresponds here to the elementary area in the phase space. The chemical potential of a particle in an aggregate is

$$\mu = \mu^0 + \frac{z}{2}\Delta F_p + RT \ln\left(\frac{A_w}{\Lambda^2}\right). \quad (22)$$

The chemical potential of a singlet particle outside an aggregate is simply its translational entropy

$$\mu = \mu^0 + RT \ln(\Lambda^2 C_u). \quad (23)$$

Here, C_u is the concentration of unbounded particles suspended in solution. At equilibrium between the solid phase and the solution phase, the chemical potentials are equal

$$C_u = \frac{A_w}{\Lambda^4} e^{-z/2\beta\Delta F_p} \equiv K. \quad (24)$$

Here, we show how a reaction constant can appear in the system. It just comes from the fact that chemical potentials of particles in the solid phase or in solution are equal. In order to simplify, we have just considered the case of the equilibrium between a pure solid phase of particles and particles suspended in solution. In our experiments, the system is a bit more complicated as it consists of a series of equilibria between clusters of different sizes. In the Appendix, we explain how to treat this more complicated case. For a solution of particles of total concentration C forming aggregates of all sizes, our calculation gives this expression for the fraction of singlets

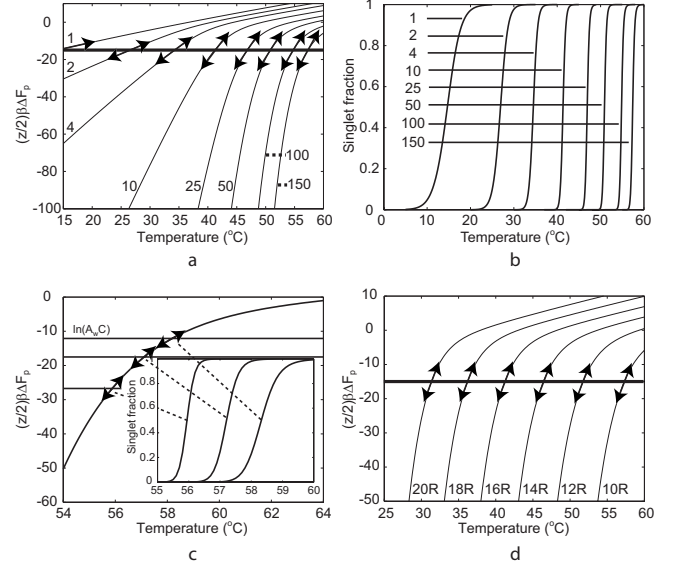


FIG. 11. (a) Particle binding free energy predicted for different coverage. Thick black line is $\ln(A_w C)$. Dissociation occurs when this line crosses the curve representing $\frac{z}{2}\Delta F_p$. $\frac{z}{2}\Delta F_p$ is plotted for seven different coverages which give the number of potential bonds indicated next to each curve. (b) Corresponding dissociation curves obtained for different coverage and therefore different numbers of potential bonds which are indicated next to the curves. (c) Influence of the wiggling area and the concentration on the dissociation temperature and on the width of the dissociation curves. (d) Particle binding free energy predicted for different entropy corrections. [(a), (c), and (d)] Arrows represent the tangent to $\frac{z}{2}\Delta F_p$ at the dissociation temperature. The slope of these arrows corresponds to the width of the transitions.

$$f = \frac{1 + 2KC - \sqrt{1 + 4KC}}{2K^2 C^2}. \quad (25)$$

From this last expression, $f = \frac{1}{2}$ for $KC = 2 - \sqrt{2} \approx 1$, dissociation occurs when the particle translational entropy difference between the singlet state and the aggregated state equals the attractive particle binding free energy mediated by the DNA. Though we have considered here the case of two-dimensional (2D) aggregates, as is the case in our experiments, these results are general and remain valid for three-dimensional (3D) aggregates. The surface concentration should be replaced by a volume concentration and the wiggling area should be replaced by a wiggling volume.

E. Dissociation and width of the transition

In Fig. 11(a), we have plotted the graph $\frac{z}{2}\beta\Delta F_p$ as a function of temperature for different particle coverages. The different coverages correspond to numbers of potential bonds varying between 1 and 150 [they are indicated on all curves in Figs. 11(a) and 11(b)]. The surface to surface separation is set to $h=L$, k is set at $k(L)$, and ΔS_p is set at $\Delta S_p \approx 10R$. In Fig. 11(a), we have also plotted the constant graph $\ln(A_w C)$ as a function of temperature for these values $A_w = 1 \text{ nm}^2$ and $C = 10^{-7} \text{ particles/nm}^2$. Dissociation occurs at the temperature where the two graphs cross. The dissociation point and

the width of the transition are actually related. The previous model allows us to predict how they are related and how they depend on parameters such as the DNA coverage on the particles and the wiggling area A_w in which a particle can move. Expanding the fraction of singlets around the dissociation temperature T_d shows that $f(T) = f(T_d) + \frac{\partial f}{\partial T}(T_d)(T - T_d)$. Therefore, the width of the transition δT is given by $\delta T^{-1} = \frac{\partial f}{\partial T}(T_d)$. Differentiating f with respect to T and taking into account that $K(T_d)C = 2 - \sqrt{2}$ leads to

$$\delta T^{-1} = A \frac{\partial(\beta\Delta F_p)}{\partial T}, \quad (26)$$

where A is a constant factor of the order of 1. According to Eq. (26), the width of the transition is given by the tangent to $\beta\Delta F_p$ at the dissociation point. Figures 11(a) and 11(b) show how the transition depends on DNA coverage. At low DNA coverage, when the number of potential bonds varies between 2 and 10, the graph $\ln(A_w C)$ (black thick solid line) crosses $\beta\Delta F_p$ (black solid line) in the “strong-binding” regime. In such a regime, the slope of the tangent to the curves is proportional to N_p . Therefore, the dissociation transition sharpens quickly as the number of tethered DNA increases [Fig. 11(b)]. Figure 11(a) also shows that for $N_p > 25$, the dissociation does not occur in the same regime: it occurs in the weak-binding regime. The width of the transition becomes very weakly dependent on the number of DNA tethered on the surface [Fig. 11(b)].

Figure 11(c) shows qualitatively the effect of the term $A_w C$ on both the dissociation temperature T_d and the width of the transition. In the “weak binding” regime, increasing $A_w C$ by increasing the wiggling area or the concentration of the particles results in increasing both the dissociation temperature and the width of the transition.

Figure 11(d) shows qualitatively the effect of the term ΔS_p on both the dissociation temperature T_d and the width of the transition. It is possible to change experimentally ΔS_p by changing the length or the type of construct which carries the sticky lengths [25]. Our calculations show that ΔS_p generates a strong temperature shift but does not change the shape of the particle binding free energy. This means that adjusting ΔS_p will allow us to adjust the dissociation temperature, but has almost no influence on the width of the transition.

IV. COMPARISON BETWEEN THEORY AND EXPERIMENTS

The theory previously developed is used to fit the data. As the repulsion interaction for our system imposes the separation between the particles at a distance $h=L$, we set the number of potential bonds $N_p = N_p(L)$ and the factor $k = k(L)$. We only leave two fitting parameters. The first parameter is the entropy correction due to the DNA tethering on the particles. The second one is the area A_w in which a particle can wiggle. The first parameter mainly shifts the dissociation temperature and has a small influence on the width of the transition, whereas the second parameter changes the width but has very little influence on the dissociation temperature. The transition is so sharp that in order to fit the width, the wig-

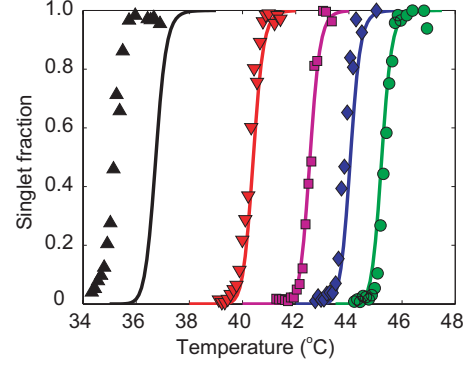


FIG. 12. (Color) Experimental and theoretical curves obtained by adjusting A_w and ΔS_p . $\gamma=0.2$ (black triangles), $\gamma=0.4$ (red inverted triangles), $\gamma=0.6$ (magenta squares), $\gamma=0.8$ (blue diamonds), $\gamma=1$ (green dots). Solid lines: results from the model.

gling area has to be set to values as small as $A_w \sim 0.2-3 \text{ nm}^2$ and the entropy correction is $\Delta S_p \sim 14.5-15.5 \text{ RJ K}^{-1} \text{ mol}^{-1}$. By setting for all the different ratios γ , $\Delta S_p = 14.55R$, and $A_w = 1 \text{ nm}^2$, we obtain the curves from Fig. 12 (solid lines). For a single set of fitting parameters, the dissociation curves are fitted very well, for both width and dissociation temperature, except for $\gamma=0.2$ where a discrepancy of $1.5 \text{ }^\circ\text{C}$ is observed between the experimental and the theoretical dissociation temperatures, which must be due to experimental error on the ratio γ or possible secondary structure formation of the sticky ends [31,33]. Otherwise, the configurational entropy cost that we find from fitting the dissociation curves is close to the $-10R$ estimated above from Eq. (13): therefore, the shift in ΔF_{tether} is therefore mostly accounted for by the entropy loss of the tethered rods. From the fitting parameters A_w , we find that $l \sim 1-4 \text{ nm}$. This value suggests that the particles are tightly packed and wiggle on a very small distance of the order of the sticky end.

V. ENGINEERING DNA-COATED COLLOIDS

This section is a short summary of the previous parts, which gives a protocol to follow in order to rationally design DNA-coated colloids with the desired dissociation transition. Once the DNA sequence is designed, the first thing to do is to characterize the experimental parameters by following the approach of Sec. II. These parameters include:

- (1) The enthalpy ΔH^0 and the entropy ΔS^0 of association of DNA in solution.
- (2) The DNA coverage on the particles.
- (3) The size and concentration of colloids.

From these factors, other factors such as the number k of DNA to which each DNA can possibly bind and the number of potential bonds N_p are inferred. The next operation to perform is to measure once a dissociation curve for one specific coverage, construct, and set of particles. From this curve, two parameters can be independently measured:

- (1) the entropic cost ΔS_p , which is adjusted to find the correct dissociation temperature;
- (2) the interaction area A_w , which is adjusted to find the correct width of the transition.

Once all these parameters are characterized, the dissociation temperature T_d and the width of the transition δT are given by

$$T_d = \frac{\Delta H^0}{\Delta S^0 + \Delta S_p - R \ln \left\{ \frac{[1 + [(2 - \sqrt{2})/A_w C]^{2/z}]^{1/N_p} - 1}{k} \right\}}, \quad (27)$$

$$\delta T^{-1} = \left(\frac{\sqrt{2} - 3}{7} \right) \left(\frac{z}{2} \right) N_p \left\{ \left[1 + \left(\frac{2 - \sqrt{2}}{A_w C} \right)^{2/z} \right]^{1/N_p} - 1 \right\} \\ \times \left(\frac{A_w C}{2 - \sqrt{2}} \right)^{2/z} \left[1 + \left(\frac{2 - \sqrt{2}}{A_w C} \right)^{2/z} \right]^{N_p - 1/N_p} \frac{\Delta H^0}{RT_d^2}. \quad (28)$$

As discussed in Sec. III, at high coverage, decreasing the number of DNA will induce a shift of the dissociation temperature toward a lower temperature but does not result in a significant change in the width of the transition. The change occurs at very low coverage, in the weak-binding regime. This also results in a slower kinetics of association [31,32]. As shown in Ref. [25], if the construct remains the same, such an approach allows us to predict the dissociation curves of aggregates where the DNA coverage and the sticky length have been changed. Reference [25] also shows that this approach remains valid for a different single-stranded DNA construct.

VI. CONCLUSION AND DISCUSSION

We have studied experimentally and theoretically the association-dissociation transition of colloids coated with complementary DNA. Two fitting parameters are extracted from the theory. The first one is the wiggling area A_w of an aggregated colloid. The second is the entropy cost experienced by hybridized tethered DNA on the surface. Once these parameters are set, the dissociation curves for different coverages are in excellent agreement with the experimental results. This finding is very useful as it shows that once A_w and ΔS_p are set for one sample of colloids, the theory can be used in predicting the desired dissociation temperature and transition widths, which are both crucial in colloidal self-assembly processes and other new fields in colloidal science such as self-replication [33].

ACKNOWLEDGMENTS

We thank J. C. Crocker, M. Clusel, and O. Gang for fruitful discussions. This work was supported by the Keck Foundation and the Nederlandse Organisatie voor Wetenschappelijk Onderzoek.

APPENDIX

The binding free energy of two particles is closely related to the binding free energy of particles inside a rigid aggregate. To calculate this binding free energy, a similar approach to that of [29,30] is taken. In a rigid aggregate, particles are considered to reside in independent ‘‘cells’’ defined by their

neighbors. In such cells, the particle can wiggle on an area A_w and interact with the neighbors, with the energy ΔF_p calculated previously. Let z be the average coordination number. The partition function for one particle in a cell Z_{cell} is

$$Z_{cell} = \frac{A_w}{\Lambda^2} e^{-z/2\beta\Delta F_p}. \quad (A1)$$

As the cells are considered to be independent and distinguishable, the total partition function Z_i for a cluster C_i containing i ($i > 1$) particles is

$$Z_{C_i} = \left(\frac{A_w}{\Lambda^2} e^{-z/2\beta\Delta F_p} \right)^i. \quad (A2)$$

The binding free energy ΔF_{C_i} of a cluster C_i becomes

$$\Delta F_{C_i} = -iRT \ln \left(\frac{A_w}{\Lambda^2} \right) + \frac{z}{2} i \Delta F_p. \quad (A3)$$

As shown in Eq. (A3), the cluster binding free energy is the sum of the binding free energies of all the interacting particles and an additional entropy correction, which corresponds to the translational entropy of particles inside their cells in the rigid cluster. To calculate the expression of the fraction of singlets as a function of temperature, the whole system of aggregates of different sizes and particles is considered as a mixture of perfect gases. Consider the ensemble of clusters C_i of i particles as a perfect gas. Let N_i be the number of clusters C_i . Its partition function $Z_{C_i,gas}$ is

$$Z_{C_i,gas} = \frac{1}{N_i!} \left(\frac{S}{\Lambda_{th,i}^2} e^{-\beta\Delta F_{C_i}} \right)^{N_i}, \quad (A4)$$

where S is the total surface of the system (or volume in three dimensions) and $\Lambda_{th,i}$ is the thermal length of a cluster of size i . This gives the following expressions for the binding free energy of the perfect gas $\Delta F_{C_i,gas}$ of clusters C_i and the chemical potential of C_i :

$$\Delta F_{C_i,gas} = N_i RT \ln([C_i] \Lambda_{th,i}^2) - N_i RT + N_i \Delta F_{C_i} \quad (A5)$$

and

$$\mu_{C_i,gas} = RT \ln([C_i] \Lambda_{th,i}^2) + \Delta F_{C_i}, \quad (A6)$$

where $[C_i] = \frac{N_i}{S}$ is the surface concentration of clusters C_i . All the clusters of different sizes follow this set of equilibria, which is verified for $i > 1$,

$$C_i + C_1 \rightleftharpoons C_{i+1} \quad \forall \quad i > 1, \quad (A7)$$

where C_1 corresponds to the singlets as a species in solution. At equilibrium, the chemical potentials follow the following condition:

$$\mu_{C_i,gas} + \mu_{C_1,gas} = \mu_{C_{i+1},gas}. \quad (A8)$$

By combining Eqs. (A3), (A6), and (A8),

$$\frac{[C_{i+1}]}{[C_i][C_1]} = \frac{\Lambda_{th,i}^2}{\Lambda_{th,i+1}^2} A_w e^{-z/2\beta\Delta F_p} \equiv K. \quad (A9)$$

Here, one recognizes the expression for the reaction constant between two particles. Its dimension is that of an area and the characteristic area A_w is the area in which a particle can wiggle inside its cell. Assuming that $\frac{\Lambda_{i,i}^2}{\Lambda_{i,i+1}^2} \simeq 1$ and that Eq. (A9) also holds for $i=1$, the reaction constant is the same for all equilibria

$$K = A_w e^{-z/2\beta\Delta F_{part}}. \quad (\text{A10})$$

As the total particle concentration is conserved

$$C = \sum_{i=1}^{\infty} i[C_i] = \frac{[C_1]}{(1 - K[C_1])^2}, \quad (\text{A11})$$

where C is the total particle concentration.

Solving Eq. (A11) gives the following expression for the fraction of singlets:

$$f = \frac{1 + 2KC - \sqrt{1 + 4KC}}{2K^2C^2}. \quad (\text{A12})$$

From this last expression, $f = \frac{1}{2}$ for $KC = 2 - \sqrt{2} \approx 1$: dissociation occurs when the particle translational entropy difference between the singlet state and the aggregated state equals the attractive particle binding free energy mediated by the DNA.

-
- [1] N. C. Seeman, *J. Theor. Biol.* **99**, 237 (1982).
 [2] N. C. Seeman, *Nature (London)* **421**, 427 (2003).
 [3] C. A. Mirkin, R. L. Letsinger, R. C. Mucic, and J. J. Storhoff, *Nature (London)* **382**, 607 (1996).
 [4] P. L. Biancaniello, A. J. Kim, and J. C. Crocker, *Phys. Rev. Lett.* **94**, 058302 (2005).
 [5] S. Y. Park, A. K. R. Lytton-Jean, S. Weigand, G. C. Schatz, and C. A. Mirkin, *Nature (London)* **451**, 553 (2008).
 [6] D. Nykypanchuk, M. M. Maye, D. van der Lelie, and O. Gang, *Nature (London)* **451**, 549 (2008).
 [7] R. C. Jin, G. S. Wu, Z. Li, C. A. Mirkin, and G. C. Schatz, *J. Am. Chem. Soc.* **125**, 1643 (2003).
 [8] V. T. Milam, A. L. Hiddessen, J. C. Crocker, D. J. Graves, and D. A. Hammer, *Langmuir* **19**, 10317 (2003).
 [9] M. P. Valignat, O. Theodoly, J. C. Crocker, W. B. Russel, and P. M. Chaikin, *Proc. Natl. Acad. Sci. U.S.A.* **102**, 4225 (2005).
 [10] A. J. Kim, P. L. Biancaniello, and J. C. Crocker, *Langmuir* **22**, 1991 (2006).
 [11] P. L. Biancaniello, J. C. Crocker, D. A. Hammer, and V. T. Milam, *Langmuir* **23**, 2688 (2007).
 [12] D. Nykypanchuk, M. M. Maye, D. van der Lelie, and O. Gang, *Langmuir* **23**, 6305 (2007).
 [13] J. M. Gibbs-Davis, G. C. Schatz, and S. T. Nguyen, *J. Am. Chem. Soc.* **129**, 15535 (2007).
 [14] M. M. Maye, D. Nykypanchuk, D. van der Lelie, and O. Gang, *Small* **3**, 1678 (2007).
 [15] N. Geerts, T. Schmatko, and E. Eiser, *Langmuir* **24**, 5118 (2008).
 [16] M. H. S. Shyr, D. P. Wernette, P. Wiltzius, Y. Lu, and P. V. Braun, *J. Am. Chem. Soc.* **130**, 8234 (2008).
 [17] H. Xiong, D. van der Lelie, and O. Gang, *Phys. Rev. Lett.* **102**, 015504 (2009).
 [18] A. J. Kim, R. Scarlett, P. L. Biancaniello, T. Sinno, and J. C. Crocker, *Nature Mater.* **8**, 52 (2009).
 [19] A. V. Tkachenko, *Phys. Rev. Lett.* **89**, 148303 (2002).
 [20] D. B. Lukatsky and D. Frenkel, *Phys. Rev. Lett.* **92**, 068302 (2004).
 [21] F. Pierce, C. M. Sorensen, and A. Chakrabarti, *Langmuir* **21**, 8992 (2005).
 [22] D. B. Lukatsky and D. Frenkel, *J. Chem. Phys.* **122**, 214904 (2005).
 [23] N. A. Licata and A. V. Tkachenko, *Phys. Rev. E* **74**, 041406 (2006).
 [24] N. A. Licata and A. V. Tkachenko, *Phys. Rev. E* **74**, 041408 (2006).
 [25] R. Dreyfus, M. E. Leunissen, R. Sha, A. V. Tkachenko, N. C. Seeman, D. J. Pine, and P. M. Chaikin, *Phys. Rev. Lett.* **102**, 048301 (2009).
 [26] J. C. Crocker and D. G. Grier, *J. Colloid Interface Sci.* **179**, 298 (1996).
 [27] J. SantaLucia, *Proc. Natl. Acad. Sci. U.S.A.* **95**, 1460 (1998).
 [28] A. K. R. Lytton-Jean and C. A. Mirkin, *J. Am. Chem. Soc.* **127**, 12754 (2005).
 [29] R. P. Sear, *Mol. Phys.* **107**, 7477 (1997).
 [30] P. Charbonneau and D. Frenkel, *J. Chem. Phys.* **126**, 196101 (2007).
 [31] M. E. Leunissen, R. Dreyfus, F. Cheong, D. G. Grier, R. Sha, N. C. Seeman, D. J. Pine, and P. M. Chaikin, *Nature Mater.* **8**, 590 (2009).
 [32] M. E. Leunissen, R. Dreyfus, R. Sha, N. C. Seeman, and P. M. Chaikin, *J. Am. Chem. Soc.* **132**, 1903 (2010).
 [33] M. E. Leunissen, R. Dreyfus, R. Sha, T. Wang, N. C. Seeman, D. J. Pine, and P. M. Chaikin, *Soft Matter* **5**, 2422 (2009).